

Evaluation of several herbal compounds as potential inhibitors of the coronavirus (COVID-19) based on virtual screening and molecular docking studies

Rezvan Marjani^{1*}

¹Department of Chemistry, Faculty of Basic Sciences, Payam Noor University, Tehran, Iran

Correspondence: Rezvan Marjani, Department of Chemistry, Faculty of Basic Sciences, Payam Noor University, Tehran, Iran, marjaniiii@yahoo.com

ABSTRACT

Researchers have tried to find a compound that can inhibit the replication of the SARS-CoV-2 virus since the outbreak of the Covid-19 pandemic. The present study evaluates the bioactive compounds found in several plants using a molecular binding approach to inhibit the primary protease of SARS-CoV-2. This study investigated 90 different herbal compounds with 8 coronavirus protein types. Auto Dock Vina 1.5.6 software was used to evaluate molecular binding. Validation was performed in PyMol software. The results were also analyzed by Biovia Discovery Studio 4.5. The best protein-ligand complex compound was selected by determining the binding score that had the highest affinity (the most negative ΔG Gibbs binding free energy). Among 90 herbal compounds, 18 herbal compounds showed high energy of -10 to -12.8 kJ/mol. Based on the results of binding energy and RMSD value, among the selected compounds, 4 compounds including Warifteine, Ginkgolide A, Emodin-8-glucoside, and Adonitoxin are recommended for further studies in the *in vivo* and *in vitro* sections.

Keywords: Coronavirus, SARS-CoV-2, Herbal compounds, Molecular binding, Auto Dock Vina

Introduction

A new respiratory viral disease was reported in Wuhan, China, in December 2019. It was an infectious disease caused by severe acute respiratory syndrome of the SARS-CoV-2 virus [1]. This disease spread worldwide, leading to an ongoing epidemic [2]. Different types of this virus have appeared in many countries until now. The most dangerous types are the alpha, beta, gamma, delta, and omicron strains [3]. About 264 million patients and more than 5 million deaths from this virus were confirmed up to December 2021, making it one of the deadliest in history [4]. Although investigations have revealed that various drugs are effective against viruses belonging to the same group, none of them has shown the same potential as a treatment for COVID-19. The primary protease of the COVID-19 virus is considered an attractive target for the study of antiviral drugs against the SARS-CoV-2 virus and other coronavirus infections. Covid-19 symptoms vary but often include fever, cough, headache, fatigue, breathing problems, and loss of smell and taste [5, 6]. This complicated situation has resulted in searching for new

treatments and rapid practical measures to treat the disease and reduce its prevalence. Hence, understanding how this virus works and spreads is vital for developing a vaccine.

Further studies are still needed to find effective drugs to inhibit the virus and specific treatment regimens to overcome morbidity and mortality since COVID-19 is a new disease with severe health problems. Covid-19 is very similar to the SARS-CoV-2 virus. There are primary five therapeutic protein targets for SARS-CoV-2, including angiotensin-converting enzyme 2 (ACE2), spike protein, major protease (M pro), RNA-dependent RNA polymerase (RdRp), and papain-like protease. In microscopic imaging, SARS-CoV-2 with its crown-like surface protrusion appears to belong to the family of beta-coronaviruses, which have encapsulated and single-stranded RNA. They primarily infect host lung cells by binding to the angiotensin-converting enzyme 2 (ACE2) receptor [7]. The surface of the COVID-19 virus contains protrusions protruding from its surface called protein spikes (Figure 1). The results of studies indicate that the COVID-19 virus uses an angiotensin-converting enzyme as a receptor to enter the cell [7]. Studies

This is an open access journal, and articles are distributed under the terms of the Creative Commons Attribution-Non Commercial-ShareAlike 4.0 License, which allows others to remix, tweak, and build upon the work non-commercially, as long as appropriate credit is given and the new creations are licensed under the identical terms.

have also revealed that the S protein of the Covid-19 virus has undergone mutations. The biological study of protein S mutations has indicated a site called RBD 1 in glycoprotein S of the virus through which it can bind to its receptor [8].

1. Receptor Binding Domain

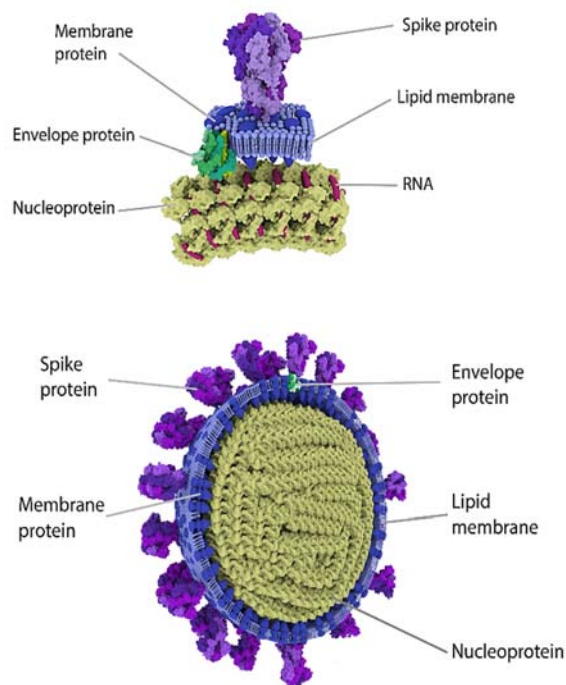


Figure 1- Structure of SARS-CoV-2 virus

Spike is the most accessible and immunogenic viral protein and thus the selected option for diagnostic and therapeutic studies [9]. Nucleocapsid protein is activated in the early stages of infection and is the most abundant protein that forms a ribonucleoprotein by binding to viral core RNA [10]. It helps RNA enter the cell and interact with cellular components. Protein N has various roles. The most significant of them include stimulating inflammation and reducing the immune response by inhibiting interferon [11]. The coat protein is a small integral membrane protein that forms ion pores across the membrane called viroporins. It is essential for virus assembly and propagation [12]. The membrane glycoprotein has a triple transmembrane domain and helps promote the spike protein [13]. The viral genome is translated as mRNA by the host cell machinery and produces enzymes necessary for RNA synthesis, including RNA-dependent RNA polymerase [14]. Then, these polyproteins are divided into structural proteins such as RdRp, M^{Pro}, and PL pro. Inhibition of M^{Pro} can block the synthesis of viral proteins. Therefore, it plays a vital role in the viral life cycle [15].

Plants are one of the sources of active medicinal compounds used extensively in the treatment of diseases [16-18]. Many reported bioactive plant compounds have antifungal, antibacterial, and

antiviral activities [19]. Plants and plant-derived products have advantages such as simplicity, greater safety, less toxicity, lower cost, higher speed of action, and compatibility with the environment compared to conventional treatment methods [20]. Drugs were extracted from natural sources in the past. These natural sources are still a major source of conductor compounds and new drugs. Nowadays, much attention is paid to pre-studies in drug design using bioinformatics methods to reduce cost and time in drug production. The use of bioinformatics tools and calculation methods that predict the effectiveness of medicinal compounds and their possible toxicity with a high confidence factor has been much considered in recent years [21]. Molecular docking, simulation, determining target point, and chemical stability studies are among the most significant bioinformatics methods used in drug design. In this regard, molecular docking plays a unique role. By considering the different states of the desired molecules in the three-dimensional space and predicting how the protein (receptor) interacts with bioactive compounds (ligand), it is possible in this technique to examine their interactions and the effective factors in the interaction and determine the more stable and important action in terms of drug identification [22]. A computational binding approach using various molecular binding software such as Auto Dock [23] provides the opportunity to identify and evaluate the bindings and efficiency of various inhibitors of natural and synthetic origin. The appropriateness of the drug can be determined by analyzing the medicinal properties after evaluating the efficient inhibitors. Although potential therapeutic agents can only be validated after experimental testing, computational binding could be a gateway to faster development of effective drugs against diseases such as COVID-19. The present study aims to find potential inhibitors of coronavirus among several selected herbal compounds that have antitussive, antipyretic, anti-viral, anti-inflammatory, antioxidant, etc. impacts using molecular docking studies. It also aims to answer the questions of whether the Covid-19 proteins can be the target of selected herbal compounds in clinical trials and what are the interactions between these proteins and the compounds.

Materials and Methods

First, the primary sequence of the 8 proteins of Covid-19 was extracted from the PDB database (Table 1). The three-dimensional structure of 90 plant compounds that had antiviral, antitussive, antipyretic, and anti-inflammatory effects were extracted from Pubchem and ChemSpider databases. Table 2 shows the characteristics of plant compounds. Then, docking was performed by Auto Dock Vina software [24]. Table 3 presents the Grid Box dimensions and its coordinates for the docking operations. Kollman Charges were used to determine the overall load. Docking results were analyzed by Biovia Discovery Studio 4.5 software [25]. The validity of the docking operation was confirmed by RMSD determination in PyMol software.

Table 1- Receptors examined in this study

Receptor	Specifications
2GIB	Crystal structure of dimerization domain of nucleocapsid protein
3VB3	Crystal structure of SARS-CoV 3C-like protease
6XHL	Covalent complex of SARS-CoV primary protease with N-[(2S)-1-((2S,3S)-3,4-dihydroxy-1-[(3S)-2-oxopyrrolidin-3-yl]butan-2-yl) 250amino)-4-methyl-1-oxopentan-2-yl]-4-methoxy-1H-indole-2-carboxamide
6Y2F	The crystal structure (monoclinic form) of the complex resulting from the reaction between the primary protease of SARS-CoV-2 (2019-nCoV) and tert-butyl (1-((S)-1-((S)-4-(benzylamino))-3,4-dioxo-1-((S)-2-oxopyrrolidin-3-yl)butan-2-yl)amino)-3-cyclopropyl-1-oxopropan-2-yl)-2-oxo-1,2-dihydropyridine-3-yl carbamate (alpha-ketoamide 13b)
7BV2	The nsp12-nsp7-nsp8 complex binds to the RNA template-primer and Remdesivir triphosphate form (RTP).
7D7K	Crystal structure of SARS-CoV-2 papain-like protease
7KAG	Crystal structure of ubiquitin-like domain 1 (Ubl1) of Nsp3 from SARS-CoV-2
7MBI	Structure of SARS-CoV2 3CL protease covalently bound to peptidomimetic inhibitor.

Table 2- Specifications of ligands studied in this study

	Plant Name	Compound Name	Molecular Formula	CID	MW
1	Arachis hypogaea	Soyasaponin I	C₄₈H₇₈O₁₈	108898*	943.1
2	Water lily	Nupharin A	C₄₁H₃₀O₂₆	8709251*	938.7
3	Green tea	4-coumaroyl-CoA	C₁₀H₁₃N₇O₁₈P₃S	4944344*	913.7
4	Periwinkle	vinblastine	C₄₆H₅₈N₄O₉	12773*	811.0
5	Lady's glove	Digoxin	C₄₁H₆₄O₁₄	2066532*	780.9
6	Cissampelos	Warifteine	C₁₆H₁₈Cl₂N₂O₆	170074	665.6
7	Forsythiae fructus	Forsythiaside A	C₂₉H₃₆O₁₅	5281773	624.6
8	Mint	Hesperidin	C₂₈H₃₄O₁₅	10621	610.6
9	Water pepper	Rutoside	C₂₇H₃₀O₁₆	5280805	610.5
10	Ginseng radix	Panasenoside	C₂₇H₃₀O₁₆	9986191	610.5
11	Ziziphi Spinosae Semen	Spinoin	C₂₈H₃₂O₁₅	155692	608.6
12	Stephania cephalantha	Cepharanthine	C₁₇H₁₈N₂O₆	10206	606.7
13	Mint	Eriocitrin	C₂₇H₃₂O₁₅	83489	596.5
14	Eriobotryae folium	-	C₂₇H₃₂O₁₄	10507459	580.5
15	Citrus reticulata	Naringin	C₂₇H₃₄O₁₄	442428	580.5
16	Chrysanthemi flos	Isorhoifolin	C₂₇H₃₀O₁₄	9851181	578.5
17	Spinach	Lutein	C₄₀H₅₆O₇	5281243	568.9
18	Boldo	-	C₁₈H₁₆N₈O₇S₄²⁻	2656	552.6
19	Pheasant's eye	Adonitoxin	C₂₉H₄₂O₁₀	441838	550.6
20	Ganoderma	Ganoderic acid C2	C₃₀H₄₆O₇	57396771	518.7
21	Rose	LNK754	C₂₉H₃₂ClN₃O₂	9805146	480.0
22	Perforate St John's-wort	-	C₂₄H₂₅F₃N₅O₃	5449447	478.5
23	Hedysarum multijugum	-	C₂₃H₃₄O₁₁	46899140	476.4
24	Azadirachta indica	Hyperoside	C₂₁H₃₀O₁₂	5281643	464.4
25	Impatiens semen	Isoquercitrin	C₂₁H₃₀O₁₂	5280804	464.4
26	Chrysanthemi flos	Thermopsoside	C₂₂H₃₂O₁₁	11294177	462.4
27	Carthami Flos	Lignan	C₂₃H₃₀O₈	261166	458.5
28	Currant	-	C₂₂H₁₈O₁₁	65064	458.4
29	Illicium Difengpi KLB Et KIM	Betulinic Acid	C₃₀H₄₈O₃	64971	456.7
30	Perilla Frutescens	Ursolic Acid	C₃₀H₄₈O₃	64945	456.7
31	Ganoderma	-	C₃₀H₄₆O₇	21635716	454.7
32	Spinach	Vitamin K	C₃₁H₄₆O₇	5280483	450.7
33	Ginseng radix	Kaempferol	C₂₁H₂₀O₁₁	5318755	448.4
34	Eriobotryae folium	Isohemiphloin	C₂₁H₃₂O₁₀	42607891	434.4
35	Myrrh	-	C₂₀H₁₈O₁₁	5317847	434.3
36	Sennae Folium	Emodin-8-glucoside	C₂₁H₃₀O₁₀	99649	432.4
37	Vitidis fructus	Vitexin	C₂₁H₃₀O₁₀	5280441	432.4
38	Oat	Vitamin E	C₂₉H₅₀O₂	14985	430.7
39	Fritillaria pallidiflora	Imperialine	C₂₇H₄₃NO₃	442977	429.6
40	Ricinus	Lupeol	C₄₀H₅₀O	259846	426.7
41	Farfarae flos	Taraxasterol	C₃₀H₅₀O	115250	426.7

42	Mori cortex	Kuwanon E	C₂₃H₂₈O₆	6440408	424.5
43	Flemingia prostrata roxb	6,8-Diprenylorobol	C₂₅H₂₆O₆	21148065	422.5
44	Gossampini flos	Mangiferin	C₁₉H₁₈O₁₁	5281647	422.3
45	Mori cortex	Kuwanon B	C₂₃H₂₄O₆	44258295	420.5
46	zingiberis	beta-sitosterol	C₂₉H₅₀O	222284	414.7
47	Soja semen nigrum	Stigmasterin	C₂₉H₄₈O	5280794	412.7
48	Jimsonweed	Ipratropium Bromide	C₂₀H₃₀BrNO₃	657308	412.4
49	Lamiaceae	Isoforskolin	C₂₇H₃₄O₇	9549169	410.5
50	Ginkgo semen	Ginkgolide A	C₂₀H₂₄O₆	9909368	408.4
51	Shepherd's Purse	Gossypetin Hexamethyl Ether	C₂₁H₃₂O₈	146093	402.4
52	Caulis piperis kadsurae	-	C₂₃H₂₈O₆	11429497	400.5
53	Colchicum autumnale	Colchicine	C₂₇H₂₅NO₆	6167	399.4
54	Ephedra	Fumaricine	C₂₁H₂₃NO₅	442236	396.4
55	Mori cortex	1,1-Diphenyl-2-Picrylhydrazine	C₁₈H₁₃N₃O₆	74358	395.3
56	Mullein	Rotenone	C₂₃H₂₂O₆	6758	394.4
57	Ginkgo semen	16-Isopropoxystrychnine	C₃₄H₃₈N₂O₃	3054016	392.5
58	Pennyroyal	Cleomiscosin A	C₂₀H₁₈O₈	442510	386.4
59	Eribotryae folium	Farnesiferol A	C₂₄H₃₀O₄	7067262	382.5
60	Magnolia flos	Veraguensin	C₂₇H₂₈O₃	443026	372.5
61	Abri herba	-	C₁₆H₁₈O₁₀	10090524	370.3
62	Trachelospermum jasminoides	Voacangine	C₂₂H₂₈N₂O₃	73255	368.5
63	Curcuma longa	Curcumin	C₂₁H₂₀O₆	969516	368.4
64	Elder	(+)-Bicuculline	C₃₀H₁₇NO₆	10237	367.4
65	Vitidis fructus	Vitetrifolin C	C₂₇H₃₇O₄	15543012	360.5
66	Tripterygii radix	Triptolide	C₂₀H₂₄O₆	107985	360.4
67	Rosemary	Rosmarinic acid	C₁₈H₁₆O₈	5281792	360.3
68	Viper's-buglosses	-	C₂₀H₂₇O₆	12309637	358.4
69	Caulis piperis kadsura	-	C₂₁H₂₆O₃	11439770	358.4
70	Papaveris pericarpium	-	C₂₇H₂₉NO₃	21287385	355.5
71	Phellodendari chinensis	D-Tetrahydropalmatine	C₂₁H₂₃NO₄	969488	355.4
72	Fumaria officinalis	Protopine	C₃₀H₁₉NO₃	4970	353.4
73	Andrographis paniculata	Andrographolide	C₂₀H₃₀O₂	5318517	350.4
74	Asteris radix Et rhizoma	-	C₂₀H₁₃NO₅	1081125	349.3
75	Knotweed	-	C₂₃H₃₀O₄	11163864	348.4
76	Arctium	Aucubin	C₁₅H₂₂O₉	91458	346.3
77	Artemisia annua	-	C₁₇H₁₄O₈	5321861	346.3
78	Cassiae Semen	Omeprazole	C₁₇H₁₉N₃O₃S	4594	345.4
79	Papaveris pericarpium	(S)-Laudanine	C₂₀H₂₅NO₄	821396	343.4
80	Tinospora cordifolia	Magnoflorine	C₂₀H₂₄NO₄[±]	73337	342.4
81	Farfae flos	-	C₁₃H₁₇N₃O₃S	9862875	342.4
82	Licorise	Glepidotin A	C₂₀H₁₈O₃	5281619	338.4
83	Hemp	Dronabinol	C₂₁H₃₀O₂	16078	314.5
84	Peucedani radix	Sesibiricin	C₂₀H₂₄O₄	12315487	328.4
85	Mallow	-	C₂₀H₂₄N₂O₂	5748152	324.4
86	Peganum harmala	Vasicinone	C₁₁H₁₀N₂O₂	442935	202.2
87	Stemona radix	-	C₈H₁₀FNO₃	9543530	198.2
88	Cordyceps	Caffeine	C₈H₁₀N₄O₂	2519	194.2
89	Orange blossom	3-Nitrosalicylic Acid	C₇H₅NO₃	6807	183.1
90	Lindens	Theobromine	C₇H₈N₄O₂	5429	180.2

*The codes are chemspider.

Table 3- The dimensions and size of the studied protein space

	center_x	center_y	center_z	size_x	size_y	size_z
2GIB	46.029	25.006	9.484	126	126	124
3VB3	11.132	0.362	23.235	126	126	126
6XHL	46.026	36.536	47.42	126	126	126
6Y2F	-4.73	-2.885	12.052	126	126	126
7BV2	97.263	98.282	99.732	126	126	126
7D7K	67.865	-36.447	2.418	126	126	126
7KAG	45.438	74.038	-0.003	118	126	126
7MBI	31.451	43.615	47.754	126	126	126

Results and Discussion

Among the 720 dockings performed, 18 plant compounds with coronavirus receptors have an energy level above -10. Tables 4

and 5 show the results whose minimum free energy is less than -10.0 Kcal/mol along with the target proteins and minimum free energy changes (ΔG) and amino acids involved in hydrogen bonding and the RMSD value of each. The results of 720 docking operations can be seen in the attached file

Table 4- Interactions and energy results of complexes higher than $\Delta G = -8.0$

Plant Name	Compound Name	Receptor	ΔG (Kcal/mol)	H - Bond	Van der waals	Pi_ Alkyl	Interactions
Lady's glove	Digoxin	7BV2	-12.8	A T:13_U P:13_A P:15_A P:14_U P:17	G P:16	A T:11	-
Arachis hypogaea	Soyasaponin I	7BV2	-12.6	A T:13_ A T:14_ U T:16_ A P:14_U P:13_C T:15_ ASN A:497_G P:16_A P:15 LEU B:287_LYS B:137_LYS	-	-	-
Lady's glove	Digoxin	3VB3	-11.7	A:5_ LEU B:271_ASP B:289_ARG B:4 A P:14_U P:12_A T:18_C	LEU B:272	MET B:276	-
Mint	Eriocitrin	7BV2	-11.7	T:15_ A T:13_ A T:14_ A T:11 VAL B:135_ALA A:7_LEU A:282_ARG A:4_LEU A:287_ASP A:289_LYS A:5_GLU B:288_SER A:284	-	U P:12	U T:12 Pi-Pi T-shaped _LYS A:500 Pi-Cation
Water lily	Nupharin A	6XHL	-11.6	U P:20_A P:19_G P:16_A T:13_C T:15_A P:14	-	ARG A:4 , LYS B:5, LYS A:5	Pi-Alkyl_ GLU B:288 , ARG A:131 ,ARG A:4,LYS A:5Pi- Anion_ARG B:4,GLU A:290 Pi-Cation
Mint	Hesperidin	7BV2	-11.4	U P:13_A T:18_ A P:14 LYS B:137_LEU A:282_GLU B:290_ASP B:289_LYS B:5_LEU B:282_GLU B:288	U P:18_ A P:19_ A T:14	U P:13_A P:14	LYS A:500 Pi-Cation
Cissampelos	Warifteine	7BV2	-11.3	U P:13_A T:18_ A P:14 LYS B:137_LEU A:282_GLU B:290_ASP B:289_LYS B:5_LEU B:282_GLU B:288	U P :12	U T:12_ A T:13	A P:14 Pi-Pi T-shaped
Arachis hypogaea	Soyasaponin I	3VB3	-11.0	U T17_U P:17_U T:12_U P:13_U P:12_G P:16_A P:14_ASN A:497_A P:15_C T:15ASN A:496	-	-	A T:13, A P:14 Pi-Pi T- shaped_ LYS A:577,U P:13 Pi-Anion
Water pepper	Rutoside	7BV2	-10.9	A T:14_U T:16_U P:18_A P:14_A P:15_A T:13 ALA C:285_SER C:284_LYS B:5_GLU B:288_ARG C:4	-	-	-
Arachis hypogaea	Soyasaponin I	7MBI	-10.8	A T:11_ ASN A:497_ASN A:496_A T:14_C T:15	U T:12	-	ARG C:4_GLY C:283_LEU B:282
Citrus reticulata	Naringin	7BV2	-10.7	LYS A:5_VAL A:125_LEU B:287	-	LYS A:5_LYS B:5_ALA A:7_ARG A:4	LYS B:5 Pi-Cation
Chrysantbemi flos	Isorhoifolin	6XHL	-10.7	A T:13_G P:10_A P:14_U P:12_A T:19_A P:11 LEU B:282_TRP B:207_THR B:285_SER A:284LEU A:282	-	-	-
Pheasant's eye	Adonitoxin	7BV2	-10.7	C T:15_ A T :14_ U P:17_G P:16_A P:19_ASN A:497	-	U T:12_ A T:11	U P:18 Pi_Pi T-Shaped
Mint	Hesperidin	3VB3	-10.6	ASN A:496_A T:13_U T:16_C T:15_A P:14_A P:15	A T:13_A T:14	-	-
Ziziphi Spinosae Semen	Spinosin	7BV2	-10.5	-	GLY B:163	LEU A:162_TYR A:264	TYR B:264 Pi_Sigma

Lady's glove	Digoxin	7D7K	-10.4	LEU B:162_TYR B:273_THR A:301	ASP B:164	-	-
Chrysanthemi flos	Isorhoifolin	3VB3	-10.4	ARG A:4_GLU A:288_VAL A:125_LYS A:5_TRP B:27_SER B:284_GLU B:288	-	LYS B:5_LYS A:5	LYS B:5 Pi-Cation
Ginseng radix	Panasenoside	7BV2	-10.3	A P:15_G P:16_U P:17_A T:11_C T:15_ASN A:496	U T:12_A P:14	-	A T:14_A T:13_U T:12 Pi_Pi T-Shaped
Myrrh	-	7BV2	-10.3	A T:13_G P:16_ASN A:497_A P:15_A P:14_U P:13_A P:14_U P:12	-	-	-
Sennae Folium	Emodin-8-glucoside	7BV2	-10.2	A P:15_G P:16_A T:13_U P:17_C T:15_U T:12	-	-	U T:12 Pi_Pi T-Shaped
Water lily	Nupharin A	3VB3	-10.1	ASP B:197_ASN B:238_ASN A:214_GLY B:138_PHE A:3_ARG A:4_ASP B:289_LEU B:287_LYS B:137	-	-	LYS B:137 Pi-Cation_ARG B:131 Pi-Anion
Forsythiae fructus	Forsythiaside A	7BV2	-10.1	U T:17_U T:16_A T:13_A T:14_A P:15_A P:14_ASN A:497	G P:16	-	-
Mint	Eriocitrin	3VB3	-10.1	SER B:284_PHE A:3_GLN B:127_ARG A:4_LYS B:5	-	LYS A:5_PHE B:291	GLU A:288 Pi-Anion
Ginkgo semen	Ginkgolide A	7BV2	-10.1	A P:15_ASN A:497_A T:13_A T:14_U P:18	-	G P:16	-
Water lily	Nupharin A	7D7K	-10.0	GLN A:269_LEU A:162_TYR B:268_TYR A:273	-	LEU A:162	TYR A:264 Pi-Pi Stacked_LYS A: 157,LYS B:157, ARG A:166 Pi-Cation
Periwinkle	vinblastine	7MBI	-10.0	GLY B:283_THR C:199	LEU C:272	-	-
Lady's glove	Digoxin	7MBI	-10.0	MET C:276_THR C:199_ALA B:285_LYS C:137	-	LEU C:284_LEU B:271_LEU B:287_MET B:276	-
Impatiens semen	Isoquercitrin	7BV2	-10.0	G P:16_A P:14_U T:12	-	-	U P:17 Pi_Pi T-Shaped

Table 5 - Validity of the data obtained from the interaction between the superior plant compounds and the proteins of the coronavirus.

Compound Name	Receptor	RMSD (A°)	Compound Name	Receptor	RMSD (A°)
Warifteine	7BV2	0.000	Eriocitrin	3VB3	1.736
Ginkgolide A	7BV2	0.000	Isorhoifolin	3VB3	1.916
Emodin-8-glucoside	7BV2	0.081	Nupharin A	7BV2	2.039
2-(3,4-dihydroxyphenyl)-5,7-dihydroxy-3-[(2R,3R,4S,5S)-3,4,5-trihydroxyoxan-2-yl]oxychromen-4-one	7BV2	0.242	Digoxin	7MBI	2.097
Soyasaponin I	3VB3	0.421	Isoquercitrin	7BV2	2.118
Adonitoxin	7BV2	0.673	Isorhoifolin	6XHL	2.278
Digoxin	3VB3	0.752	Nupharin A	7D7K	2.433
Soyasaponin I	7BV2	0.791	Isorhoifolin	7BV2	2.808
Panasenoside	7BV2	1.116	Forsythiaside A	7BV2	3.052
Eriocitrin	7BV2	1.144	Digoxin	7D7K	3.281
Soyasaponin I	7MBI	1.258	Digoxin	7BV2	3.293
Naringin	7BV2	1.300	vinblastine	7MBI	3.461
Spinosin	7BV2	1.338	vinblastine	7D7K	3.579
Hesperidin	3VB3	1.451	Rutoside	7BV2	3.812
Nupharin A	3VB3	1.465	Hesperidin	7BV2	5.161
Nupharin A	6XHL	1.700			

A minimum number of hydrogen bonds must be formed for the pseudo-drug to affect the receptor [26] and the RMSD value is used to confirm the binding protocol. Thus, results without hydrogen bonds and RMSD values above 1.5 angstroms in Table 5 were omitted, despite having the highest delta G values. Table 4 presents 21 compounds. Based on the molecular docking studies, 18 compounds including Digoxin, Soyasaponin I, Eriocitrin, Nupharin A, Hesperidin, Rutoside, Naringin, Warifteine, Isorhoifolin, Adonitoxin, Spinosin, Panasenoside, vinblastine, Emodin-8-glucoside, Ginkgolide A, Forsythiaside, Isoquercitrin, 2-(3,4-dihydroxyphenyl)-5,7-dihydroxy-3-[(2R,3R,4S,5S)-3,4,5-trihydroxyoxan-2-yl]oxychromen-4-one had binding free energy above -10 Kcal/mol and had a good interaction with 7BV2, 3BV3, 6XHL, 7MBI, and 7D7K proteins of coronavirus.

Based on Table 5, which validates the obtained data, 18 compounds are presented. Eight compounds among them showed the best RMSD results, indicating the validity of the data of this study. Digoxin compound in binding with 7BV2 receptor did not have an acceptable RMSD value despite the best binding energy. Warifteine and Ginkgolide A compounds caused protein instability by binding to 7BV2, which can be seen in RMSD analysis. The RMSD obtained from this compound is zero Å° (Figures 2 and 3), indicating the validity of the binding protocol. These compounds are not toxic [27, 28].

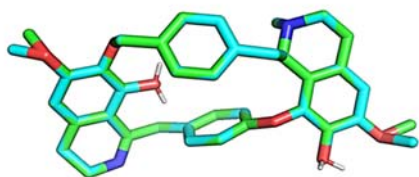


Figure 2- RMSD of Å°0.0 for the Warifteine Cissampelos compound by Pymol software

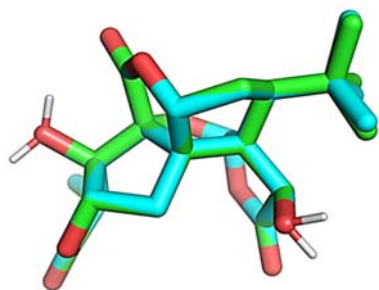


Figure 3- RMSD of Å° 0.0 for the Ginkgolide A compound of the Ginkgo semen by Pymol software

Soyasaponin I found in *Arachis hypogaea* in interaction with protein 7BV2 with binding free energy of 6.12-Kcal/mol has established a hydrogen bond with A T:13_ A T:14_ U T:16_ A P:14_ U P:13_ C T:15_ ASN A:497_ G P :16_ A P:15 amino acids (Figure 4).

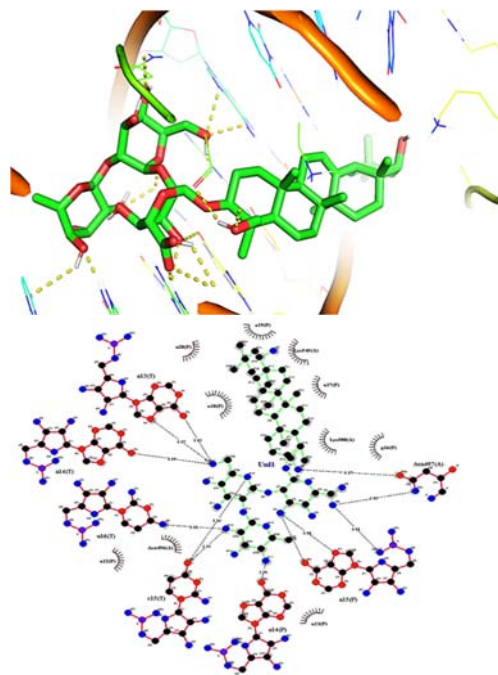


Figure 4- The interaction of 7BV2 protein and Soyasaponin I compound

The compound of Digoxin found in the Lady's glove in interaction with the 3BV3 protein with a binding free energy of -7.11 Kcal/mol has established a hydrogen bond with LEU B:287_LYS B:137_LYS A:5_ LEU B:271_ASP B:289_ARG B:4 amino acids and a van der Waals interaction with LEU B:272 amino acid, and Pi - Alkyl interaction with MET B:276 amino acid (Figure 5).

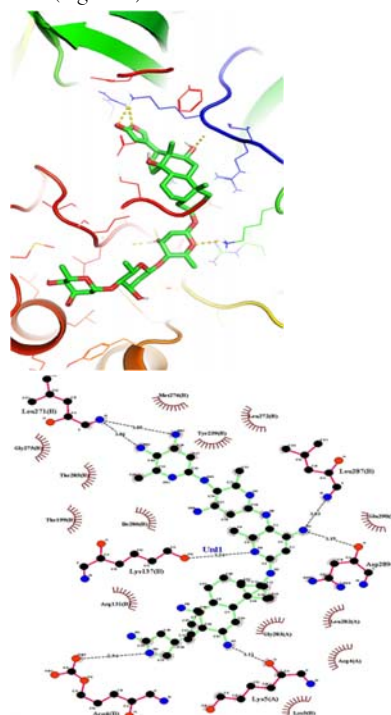


Figure 5- The interaction of 3BV3 protein and Digoxin compound

Warifteine compound found in the *Cissampelos* plant in interaction with 7BV2 protein with binding free energy of 3.11-Kcal/mol has established a hydrogen bond with U P:13_A T:18_A P:14 amino acids, van der Waals interaction with amino acid U P:12, Pi - Alkyl interaction with acid Aminos U T:12-A T:13, and a Pi-Pi T-shaped interaction with A P:14 amino acid (Figure 6).

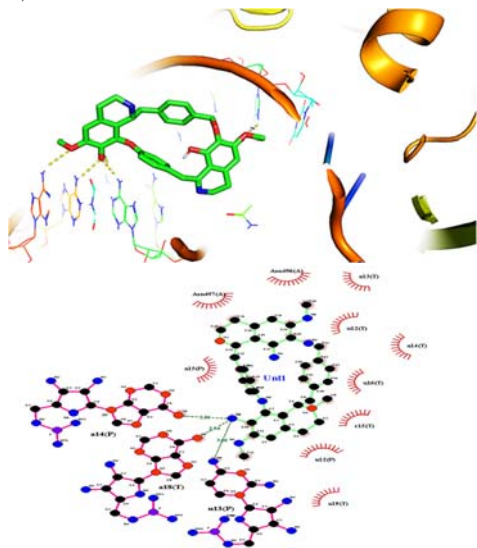


Figure 6- The interaction of 7BV2 protein and Warifteine compound

Soyasaponin I found in *Arachis hypogaea* in interaction with 3BV3 protein with the binding free energy of -0.11 Kcal/mol has established a hydrogen bond with amino acids _LYS B:137_LEU A:282_GLU B:290_ASP B:289_LYS B:5_LEU _B:282_GLU B:288 and a van der Waals interaction with SER A:284 amino acid (Figure 7).

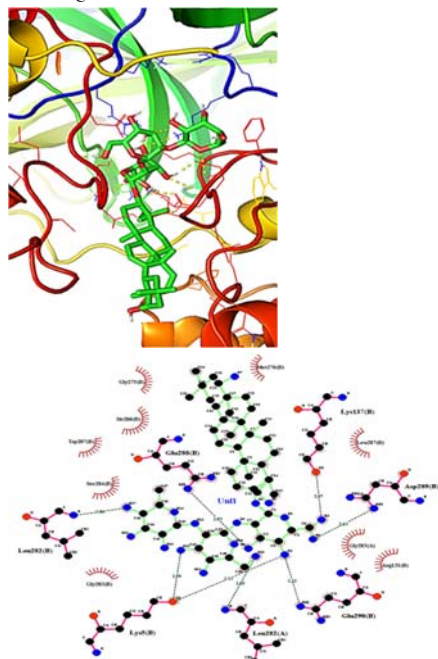


Figure 7- The interaction of 3BV3 protein and Soyasaponin I compound

The Adonitoxin compound found in the Pheasant's eye plant in the interaction with the 7BV2 protein with a binding free energy of 7.10-Kcal/mol has established a hydrogen bond with G P:10_A T:14_A P:14_U P:12_A T:19_A P:11 amino acids (Figure 8).

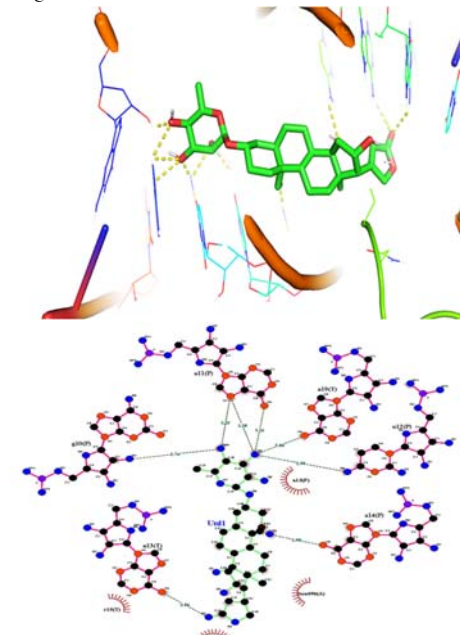


Figure 8- The interaction of 7BV2 protein and Adonitoxin compound

2-(3,4-dihydroxyphenyl)-5,7-dihydroxy-3-[(2R,3R,4S,5S)-3,4,5-trihydroxyoxan-2-yl] oxychromen-4-one compound found in the Myrrh plant in interaction with the 7BV2 protein with a binding free energy of -3.10 Kcal/mol has established a hydrogen bond with A T:13_P:16_ASN A:497_A P:15_A P:14_U P:13_U P:12_A T:14_G amino acids (Figure 9).

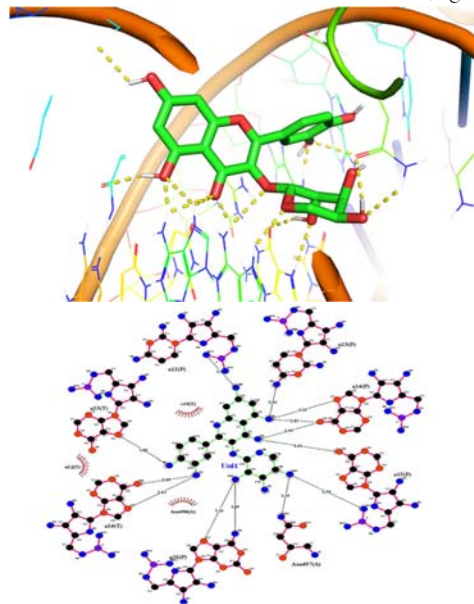


Figure 9- On the interaction of 7BV2 protein and the composition in myrrh plant

Emodin-8-glucoside compound found in *Sennae Folium* plant in interaction with 7BV2 protein with binding free energy of 2.10-Kcal/mol has established a hydrogen bond with P:15_G P:16_A T:13_C T:15_U P:17_U T:12 amino acids and a Pi-Pi T-shaped interaction with U T:12 amino acid (Figure 10).

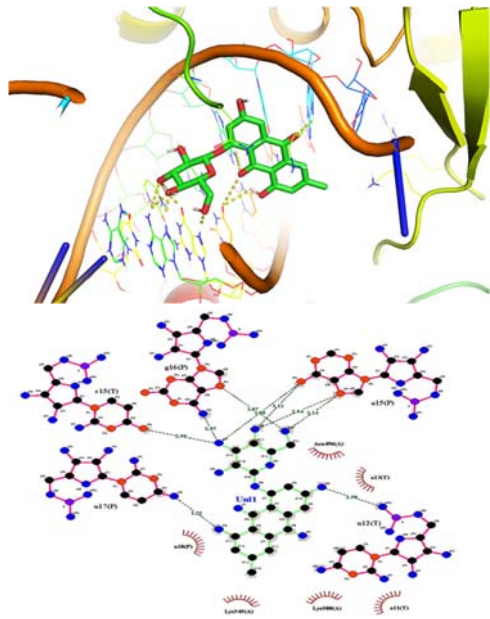


Figure 10- The interaction of 7BV2 protein and Emodin-8-glucoside compound

The Ginkgolide A compound found in the Ginkgo semen in interaction with the 7BV2 protein with a binding free energy of -1.10 Kcal/mol has established a hydrogen bond with A P:15_ASN A:497_A T:13_A T:14_U P:18 amino acids and a Pi-Alkyl interaction with G P 16 amino acid (Figure 11).

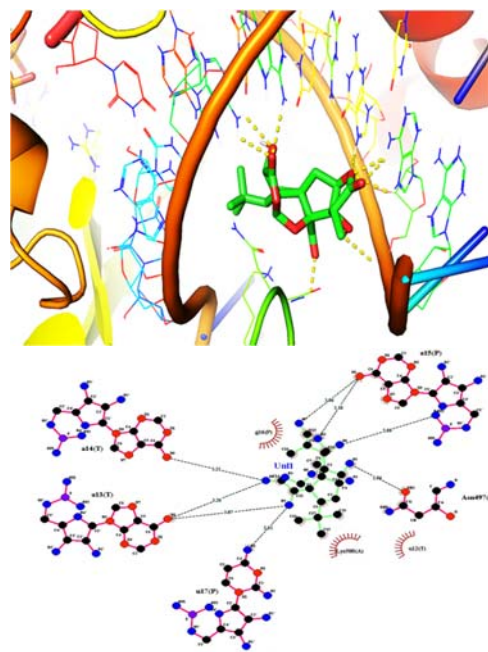


Figure 11- The interaction of 7BV2 protein and Ginkgolide A compound

Several different classes of bioactive molecules isolated from many plants have antiviral activity [28-30]. One method of determining whether a compound has medicinal potential is to follow Lipinski's rule of five (RO5). Based on this rule, orally active drugs should not violate more than one of the set criteria [31]. Thus, it was investigated whether each docking compound corresponds to Lipinski's RO5. Some compounds that violate RO5 are 2-(3,4-dihydroxyphenyl)-5,7-dihydroxy-3-[(2R,3R,4S,5S)-3,4,5-trihydroxyoxan-2-yl]oxychromen-4-one, and Soyasaponin I and Digoxin (Table 6).

Table 6- Review of Lipinski's RO5 of superior compounds

Compound Name	mass	hydrogen bond donor	hydrogen bond acceptors	Log P
Warifteine	558	2	7	1.10
Ginkgolide A	386	2	9	0
Emodin-8-glucoside	418	6	10	-0.66
2-(3,4-dihydroxyphenyl)-5,7-dihydroxy-3-[(2R,3R,4S,5S)-3,4,5-trihydroxyoxan-2-yl]oxychromen-4-one	423	7	11	-0.93
Soyasaponin I	875	11	18	1.99
Adonitoxin	513	5	10	0
Digoxin	722	6	14	0

Ligands binding to the active site of this receptor can significantly inhibit receptor function. Ligand interactions that have the least binding affinity were Digoxin, Soyasaponin I, Eriocitrin, Nupharin A, Hesperidin, Rutoside, Naringin, Warifteine, Isorhoifolin, Adonitoxin, Spinoin, Panasenoside, vinblastine, Emodin-8-glucoside, Ginkgolide A, Forsythiaside, Isoquercitrin and 2-(3,4-dihydroxyphenyl)-5,7-dihydroxy-3-[(2R,3R,4S,5S)-3,4,5-trihydroxyoxan-2-yl]oxychromen-4-one. They showed that the ligand is precisely bound to the active sites in the form of hydrogen and van der Waals bonds. The bond will be stronger when more hydrogen bonds with amino acid residues. This makes the energy score lower and the bonds more stable. Glycoside compounds such as flavonol glycoside have therapeutic properties including treating headache, and fever, and helping to treat cough, bronchitis, and infectious diseases. [32]. Binding scores of glycosidic compounds Digoxin, Eriocitrin, Hesperidin, Naringin, Adonitoxin, Spinoin and 2-(3,4-dihydroxyphenyl)-5,7-dihydroxy-3-[(2R,3R,4S,5S)-3,4,5-trihydroxyoxan-2-yl]oxychromen-4-one and Emodin-8-glucoside with 7BV2 protein were -8.12, -7.11, -4.11, -7.10, -7.10, -5.10, -3.10, and -2.10, respectively. The results of studies by Otomo *et al.* [33], Chen *et al.* [34], and Adam *et al.* [35] confirm some of these results.

Based on Lin *et al.*'s experiments, the Emodin-8-glucoside compound has very good water solubility and shows almost no cytotoxicity [36]. Animals that consume plants containing cardiac glycosides, including Adonitoxin, mostly suffer from fatal digestive and cardiac disorders despite the antioxidant, antimicrobial, anti-inflammatory, cardioprotective, neuroprotective, and antiallergic properties of glycosidic compounds [37]. However, recent studies have indicated that using a low dose of this compound has therapeutic properties. In short, phytochemical and pharmacological studies of the Adonis L. genus have received much attention [38, 39]. Extracts enriched in cardiac glycosides have been made and the active compounds have been isolated and proven to provide cardioprotective activity. However, plants of this genus should be further studied and developed with special attention to resource conservation and clinical trials. Terpenoids are active compounds found in plants. The binding score of Soyasaponin I against the primary protease was -12.6. This compound also has anti-inflammatory activity in addition to being known as a herpes simplex virus [40], [41]. However, some studies indicate that this compound can increase the pathogenicity of the virus to the host [41, 42]. Warifteine and Nupharin A are alkaloid compounds with binding scores of -3.11 and -0.11, respectively, which have the properties of treating asthma, inflammatory disorders, bronchitis, antiplatelet and anticoagulant [43].

Conclusion

This study revealed that the natural compounds 2-(3,4-dihydroxyphenyl)-5,7-dihydroxy-3-[(2R,3R,4S,5S)-3,4,5-trihydroxyoxan-2-yl]oxychromen-4-one, Soyasaponin I, Digoxin, Eriocitrin, Nupharin A, Hesperidin, Rutoside,

Naringin, Panasenoside, and Isorhoifolin have better binding free energies with the 7BV2 protein of SARS-CoV-2 among the selected proteins of the coronavirus. Although the molecular binding results of Warifteine, Ginkgolide A, Emodin-8-glucoside, and Adonitoxin are not as good as those compounds, the analysis of RMSD parameters, interactions, number of hydrogen bonds, and RO5 criteria, and their non-toxic properties showed better performance. These compounds have a better potential as antiviral plant chemicals and to solve respiratory, inflammatory, infectious, and coagulation problems, which may prevent the proliferation of the virus or help to treat this disease. It can be stated that these 4 inhibitors are appropriate candidates as drugs for inhibiting the activity of the primary enzyme of the SARS-CoV-2 coronavirus for clinical and laboratory studies. However, the conducted studies are theoretical. Experimental work is required to ensure the accuracy of the data and the results of this study alone cannot claim that the introduced compounds can inhibit the protease of Covid-19.

Acknowledgments: Author would like to sincerely thank the Dr. Masoud Mandoioe for their support during completion of this study.

Conflict of interest: The author declares that she has no competing financial interests or known personal relationships that would appear to influence the work reported in this article

Financial support: None **Ethics statement:** None

References

1. Sherif, Y.E., *et al.* (2021), Phytochemicals of Rhus spp. as potential inhibitors of the SARS-CoV-2 main protease: molecular docking and drug-likeness study. Evidence-Based Complementary and Alternative Medicine, 2021.
2. Zimmer, C. (2021), The Secret Life of a Coronavirus—An oily, 100-nanometer-wide bubble of genes has killed more than two million people and reshaped the world. Scientists don't quite know what to make of it. Scientists don't quite know what to make of it. Retrieved, 28.
3. Cedro-Tanda, A., *et al.* (2021), The evolutionary landscape of SARS-CoV-2 variant B. 1.1. 519 and its clinical impact in Mexico City. *Viruses*, 13(11): p. 2182.
4. COVID, G. (2021), database Retrieved from <https://github.com/CSSEGISandData/COVID-19>.
5. Saniasiaya, J. (2019), M.A. Islam, and B. Abdullah, Prevalence of olfactory dysfunction in coronavirus disease (COVID-19): a meta-analysis of 27,492 patients. *The Laryngoscope*, 2021. 131(4): p. 865-878.

- .6 Agyeman, A.A. (2020), et al. Smell and taste dysfunction in patients with COVID-19: a systematic review and meta-analysis. in Mayo Clinic Proceedings.. Elsevier.
- .7 Li, W., et al. (2003), Angiotensin-converting enzyme 2 is a functional receptor for the SARS coronavirus. *Nature*, 426(6965): p. 450-454.
- .8 Ramsey, I., N. Spibey ,and O. Jarrett. (1998),The receptor binding site of feline leukemia virus surface glycoprotein is distinct from the site involved in virus neutralization. *Journal of virology*, 72(4): p. 3268-3277.
- .9 Zhou, P., et al. (2020), A pneumonia outbreak associated with a new coronavirus of probable bat origin. *nature*, 579(7798): p. 270-273.
- .10 Huang, Q., et al. (2004), Structure of the N-terminal RNA-binding domain of the SARS CoV nucleocapsid protein. *Biochemistry*, 43(20): p. 6059-6063.
- .11 Lu, X., et al. (2011), SARS-CoV nucleocapsid protein antagonizes IFN- β response by targeting initial step of IFN- β induction pathway, and its C-terminal region is critical for the antagonism. *Virus genes*, 42(1): p. 37-45.
- .12 Satarker, S. and M. Nampoothiri,(2020), Structural proteins in severe acute respiratory syndrome coronavirus-2. *Archives of medical research*, 51(6): p. 482-491.
- .13 Neuman, B.W., et al. (2011), A structural analysis of M protein in coronavirus assembly and morphology. *Journal of structural biology*, 174(1): p. 11-22.
- .14 Poduri, R., G. Joshi, and G. Jagadeesh, (2020), Drugs targeting various stages of the SARS-CoV-2 life cycle: Exploring promising drugs for the treatment of Covid-19. *Cellular signalling*, 74: p. 109721.
- .15 Rathnayake, A.D., et al. (2020), 3C-like protease inhibitors block coronavirus replication in vitro and improve survival in MERS-CoV–infected mice. *Science translational medicine*, 12(557): p. eabc5332.
- .16 Shakeran, Z., M. Nosrati, and Z. Shakeran. (2018), In silico screening of hepatitis C virus NS3/4A protease inhibitor (s) from *Cornus officinalis* and *Syzygium aromaticum*.
- .17 Mustafa, S., H. Balkhy, and M. Gabere. (2019), Peptide-protein interaction studies of antimicrobial peptides targeting middle east respiratory syndrome coronavirus spike protein :an in silico approach. *Advances in bioinformatics*, 2019.
- .18 Shakeran, Z., M. Nosrati, and Z. Shakeran. (2018), In silico Screening of Hepatitis C Virus NS3/4A Protease Inhibitor (s) from medicinal plants. *Razi Journal of Medical Sciences*, 25(167): p. 69-80.
- .19 Cheng, P.W., et al. (2006), Antiviral effects of saikosaponins on human coronavirus 229E in vitro. *Clinical and Experimental Pharmacology and Physiology*, 33(7): p. 612-616.
- .20 Ameer, K., H.M. Shahbaz, and J.H. (2017), Kwon, Green extraction methods for polyphenols from plant matrices and their byproducts: A review. *Comprehensive Reviews in Food Science and Food Safety*, 16(2): p. 295-315.
- .21 Nantasenamat, C., C. Isarankura-Na-Ayudhya, and V. Prachayasittikul. (2010), Advances in computational methods to predict the biological activity of compounds. *Expert opinion on drug discovery*, 5(7): p. 633-654.
- .22 Ferreira, L.G., et al. (2015), Molecular docking and structure-based drug design strategies. *Molecules*, 20(7): p. 13384-13421.
- .23 Morris, G.M., et al. (2001), AutoDock. Automated docking of flexible ligands to receptor-User Guide.
- .24 Huey, R., G.M. Morris, and S. Forli. (2012), Using AutoDock 4 and AutoDock vina with AutoDockTools: a tutorial. The Scripps Research Institute Molecular Graphics Laboratory, 1055 :p. 92037.
- .25 Studio, D.(2015), Dassault systemes BIOVIA, Discovery studio modelling environment, Release 4.5. Accelrys Softw Inc, 2015: p. 98-104.
- .26 Chen, D., et al. (2016), Regulation of protein-ligand binding affinity by hydrogen bond pairing. *Science advances*, 2(3): p. e1501240.
- .27 Barbosa Filho, J.M., M.d.F. Agra, and G.(1997), Thomas, Botanical, chemical and pharmacological investigation on *Cissampelos* species from Paraíba (Brazil). *Ciênc. cult.(São Paulo)*, 1997: p. 386-94.
- .28 Ullah, S., et al. (2022), Identification of phytochemical inhibitors of SARS-CoV-2 protease 3CLpro from selected medicinal plants as per molecular docking, bond energies and amino acid binding energies. *Saudi Journal of Biological Sciences*, 29(6): p. 103274.
- .29 Mukhtar, M. ,et al. (2008), Antiviral potentials of medicinal plants. *Virus research*, 131(2): p. 111-120.
- .30 Denaro, M., et al. (2020), Antiviral activity of plants and their isolated bioactive compounds: An update. *Phytotherapy Research*, 34(4): p. 742-768.
- .31 Lipinski, C.A., et al. (1997), Experimental and computational approaches to estimate solubility and permeability in drug discovery and development settings. *Advanced drug delivery reviews*, 23(1-3): p. 3-25.
- .32 Brett, G.M., et al. (2008), Absorption, metabolism and excretion of flavanones from single portions of orange fruit and juice and effects of anthropometric variables and contraceptive pill use on flavanone excretion. *British Journal of Nutrition*, 101(5): p. 664-675.
- .33 Utomo, R.Y., M. Ikawati, and E. (2020), Meiyanto, Revealing the potency of citrus and galangal constituents to halt SARS-CoV-2 infection.
- .34 Chen, Y.W., C.-P.B. Yiu, and K.-Y.(2020), Wong, Prediction of the SARS-CoV-2 (2019-nCoV) 3C-like protease (3CL pro) structure: virtual screening reveals velpatasvir, ledipasvir, and other drug repurposing candidates. *F1000Research*, 9.
- .35 Adem, S., et al.(2020), Identification of potent COVID-19 main protease (Mpro) inhibitors from natural

polyphenols: an in silico strategy unveils a hope against CORONA.

.36 Lin, H.-W., et al.(2010), Anti-HIV activities of the compounds isolated from *Polygonum cuspidatum* and *Polygonum multiflorum*. *Planta medica*, 76(09): p. 889-892.

.37 Galey, F.D., et al.(1996), Diagnosis of oleander poisoning in livestock. *Journal of Veterinary Diagnostic Investigation*, 8(3): p. 358-364.

.38 Zhang, L.-h., et al.(2015), Determination of other related carotenoids substances in astaxanthin crystals extracted from *Adonis amurensis*. *Journal of Oleo Science*, 64(7): p. 751-759.

.39 Shang, X., et al.(2019), The genus *Adonis* as an important cardiac folk medicine: a review of the ethnobotany,

phytochemistry and pharmacology. *Frontiers in Pharmacology*, 10: p. 25.

.40 Blevins, R.D. and M.P. (1980), Domic, The effect of Δ -9-tetrahydrocannabinol on herpes simplex virus replication. *Journal of General Virology*, 49(2): p. 427-431.

.41 Reiss, C.S. (2010), Cannabinoids and viral infections. *Pharmaceuticals*, 3(6): p. 1873-1886.

.42 Tahamtan, A., et al. (2018), Effects of cannabinoid receptor type 2 in respiratory syncytial virus infection in human subjects and mice. *Virulence*, 9(1): p. 217-230.

.43 Roberts, M.F.(2013), Alkaloids: biochemistry, ecology, and medicinal applications. Springer Science & Business Media.